



Bocus, J., Doufexi, A., & Agrafiotis, D. (2019). MU-Massive MIMO for UWA Communication. In *2018 IEEE 88th Vehicular Technology Conference (VTC-Fall 2018): Proceedings of a meeting held 27-30 August 2018, Chicago, Illinois, USA* (pp. 1754-1758). [8690941] Institute of Electrical and Electronics Engineers (IEEE).
<https://doi.org/10.1109/VTCFall.2018.8690941>

Peer reviewed version

License (if available):
Other

Link to published version (if available):
[10.1109/VTCFall.2018.8690941](https://doi.org/10.1109/VTCFall.2018.8690941)

[Link to publication record in Explore Bristol Research](#)
PDF-document

This is the accepted author manuscript (AAM). The final published version (version of record) is available online via IEEE at <https://doi.org/10.1109/VTCFall.2018.8690941> . Please refer to any applicable terms of use of the publisher.

University of Bristol - Explore Bristol Research

General rights

This document is made available in accordance with publisher policies. Please cite only the published version using the reference above. Full terms of use are available:
<http://www.bristol.ac.uk/pure/about/ebr-terms>

MU-Massive MIMO for UWA Communication

Mohammud J. Bocus, Angela Doufexi, Dimitris Agrafiotis

Department of Electrical and Electronic Engineering, University of Bristol, BS8 1UB, UK.

Abstract—The present paper considers the application of massive multiple-input multiple-output (MIMO) to a multi-user (MU) underwater acoustic (UWA) communication system. In the scope to achieve a high throughput within a limited acoustic bandwidth, we consider filterbank multicarrier (FBMC) modulation for waveform shaping instead of the widely used orthogonal frequency division multiplexing (OFDM). We assess the performance of the system in a 1 km simulated time-varying underwater acoustic channel (UAC) in terms of bit error rate (BER), packet error rate (PER) and maximum achievable throughput. The transmission scenario consists of four users, each one equipped with multiple transmitting hydrophones. We show that the implementation of massive MIMO at the receiver allows all the users to use the same frequency bandwidth to transmit their information reliably to the receiver. Therefore, a high spectral efficiency and throughput can be achieved, making the transmission of multimedia data such as high quality real-time video a reality.

I. INTRODUCTION

In recent years, underwater communication has drawn interest from many sectors due to a growing number of applications such as sea exploration, video-assisted navigation, pollution monitoring, offshore oil and gas extraction, military defense and surveillance, seismic monitoring among many others. Most of these applications usually require real-time video transmission with acceptable video quality but this represents a challenge due to frequency-dependent attenuation and ambient noise which make the UWA bandwidth very limited [1]. Furthermore, for some time-critical applications, multiple remotely operated underwater vehicles (ROVs) which transmit their data concurrently to a surface vessel need to be deployed.

Single user (SU) MIMO technology has been successfully applied to UWA communication to cope with the increase in data traffic in modern underwater applications. However, this technology on its own does not provide much benefits in an UAC. This is because the UAC (especially a shallow water horizontal channel) is severely affected by multipath distortion and the delay spread can span over tens to even hundreds of milliseconds due to the low speed of sound in water [1]. In this regard, OFDM has been integrated with MIMO to provide robust performance against inter-symbol interference (ISI), ensure simple one-tap frequency domain equalization and at the same time provide an increase in data rate and better system reliability (e.g., [2]–[4]). OFDM, however, does not provide the most optimum solution to meet the throughput demand for underwater applications that generate high traffic data. This is because in OFDM, the cyclic prefix (CP) carries redundant information and therefore represents a wastage of bandwidth resources. Furthermore, in order to cope with the extended channel impulse response (CIR) in UACs, the duration of the CP and consequently the OFDM symbol should be increased

to preserve the bandwidth efficiency [5]. The problem that may arise in fast varying UACs is that Doppler distortion caused by motion may cause severe inter-carrier interference (ICI) in the OFDM system and hence degrade its performance.

One technique that can overcome the drawbacks of OFDM in an UAC and simultaneously improve the bandwidth efficiency is FBMC. The prototype filter can be optimized in such a way that the subcarriers have excellent frequency localization and therefore FBMC can provide robust performance in doubly-dispersive channels without using any CP [6]. Cosine modulated multitone (CMT) and filtered multitone (FMT)-based FBMC systems have been investigated for UWA communication where good performance has been achieved [7], [8]. However, the authors considered a SU scenario with a single transmitting transducer and multiple receiving hydrophones.

Massive MIMO technology has only been recently proposed to improve the throughput and reliability in UWA communication systems. For instance in [5], a CMT-based massive MIMO system is suggested for UACs to enhance the bandwidth efficiency. In this scenario, an underwater base-station (BS) equipped with a large number of receiving hydrophones is considered and four transmitting nodes are assumed, each one equipped with a single loudspeaker. In an effort to efficiently track channel variations using a blind equalization method based on the constant modulus algorithm (CMA), only 32 subcarriers were used for a small system's bandwidth of 5 kHz (and carrier frequency of 8 kHz). Each user transmits a total of 8 bits of coded information/s/Hz simultaneously to the array of receiving hydrophones over a distance of 1 km and water depth of 30 m. Simulation results showed that by increasing the number of hydrophones at the BS from 20 to 100, the signal-to-interference-plus-noise ratio (SINR) for each user could be improved from approximately 12 dB to 18 dB. Furthermore, the absence of pilots for channel estimation resulted in a bandwidth efficiency as high as 8 b/s/Hz.

In this work we propose to use a MU-massive MIMO system for UWA communication where the users are equipped with multiple transmitting hydrophones. To make maximum use of the available bandwidth, we use the Offset Quadrature Amplitude Modulation (OQAM)-based FBMC system. However, it is well-known that the FBMC/OQAM system suffers from imaginary interference since the complex orthogonality no longer holds. This shortcoming of FBMC/OQAM also makes channel estimation and MIMO integration challenging. Therefore, in this work we use a low-complexity modified FBMC/OQAM system as proposed in [9] where complex symbols can be either spread in time or frequency [10] to eliminate the imaginary interference. We assess the performance of the Turbo-coded

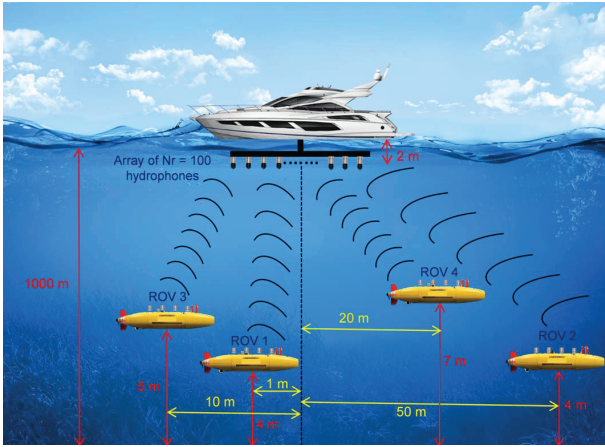


Fig. 1. MU-massive MIMO UWA transmission scenario

system over a simulated 1 km time-varying UAC in terms of BER, PER and maximum achievable throughput.

The rest of this paper is organized as follows. Section II introduces our transmission scenario in the UAC. Section III gives a brief overview of the UAC characteristics since they are widely available in literature (e.g., [1], [11]). Section IV provides an overview of the modified FBMC/OQAM system used in this work. The system model for a massive MIMO system is described in Section V. Our system's performance is evaluated using numerical simulations in Section VI. Finally, concluding remarks are drawn in Section VII.

Notation. $(\cdot)^T$ and $(\cdot)^H$ denote the transpose and Hermitian transpose operations respectively. \mathbf{I} is an identity matrix.

II. TRANSMISSION SCENARIO

The MU-massive MIMO setup considered in this work is depicted in Fig. 1. The BS receiver array consists of 100 receiving hydrophones which can be attached to a surface vessel such as a ship or oil platform. Four ROVs are deployed at various depths and separation distances and each one is equipped with four transmitting hydrophones. The ROVs transmit their data simultaneously to the surface vessel in the uplink while the BS transmit control information to each ROV in the downlink. In order to provide adequate spacial resolution in the massive MIMO system, the separation between the hydrophones should be greater than half the wavelength [5]. Hence, assuming a carrier frequency of 32.5 kHz and a nominal speed of sound of 1500 m/s, the minimum hydrophone spacing is equal to 2.3 cm. This scenario can be of interest in the offshore oil and gas industry to carry out time-critical maintenance or intervention work on sub-sea infrastructure. This underwater communication scenario can also allow a larger search area to be covered on the ocean floor when looking for sunken objects.

III. UAC OVERVIEW

Unlike terrestrial links, the challenges involved in UWA communication are quite different. The type of water (freshwater or sea water), depth, temperature, pH, salinity, impurities and water composition all affect the acoustic wave propagation.

Not only we have to consider these factors but we have to take into account common terrestrial phenomena such as frequency-dependent attenuation, multipath propagation which is caused by reflection (in shallow water) and refraction (mostly observed in deep water propagation), Doppler effect and noise. However, as compared to terrestrial links, the multipath delay spread in an UAC is usually in the order of milliseconds and this can result in severe frequency-selective signal distortion [1]. Furthermore, due to the low speed of sound as compared to electromagnetic waves, motion-induced Doppler distortion is non-negligible. Noise in an UAC usually consists of ambient noise (caused by turbulence, breaking waves, rain, and distant shipping) and site-specific noise (ice cracking, snapping shrimps, etc) [1]. Ambient noise has a decaying power spectral density and is usually predominant at very low frequencies. The attenuation and ambient noise severely limit the acoustic bandwidth and hence the latter is usually in the order of a few kHz for long transmission distances (above 1 km).

IV. INTERFERENCE CANCELLATION IN FBMC/OQAM

In a conventional FBMC/OQAM system, maximum bandwidth efficiency can be achieved at the expense of intrinsic imaginary interference. The authors in [9] devised a low-complexity method to cancel the imaginary interference such that all MIMO signal processing known in OFDM can be straightforwardly applied. The method consists of spreading the symbols in the time domain using a coding procedure and in so-doing the complex orthogonality can be restored. For an FBMC/OQAM system consisting of L subcarriers and K time symbols, the transmitted signal is generated as [9]

$$s(t) = \sum_{k=1}^K \sum_{l=1}^L g_{l,k}(t) x_{l,k}, \quad (1)$$

where $x_{l,k}$ denotes the real-valued symbol transmitted on subcarrier position l and time position k , and $g_{l,k}(t)$ is the time and frequency shifted version of a prototype filter $p(t)$:

$$g_{l,k}(t) = p(t - kT) e^{j2\pi lF(t-kT)} e^{j\frac{\pi}{2}(l+k)}, \quad (2)$$

where T and F denote the time and subcarrier spacings respectively. In FBMC/OQAM, $p(t)$ is only orthogonal for $TF = 2$. To make the data rate similar to OFDM (without CP), the time and frequency spacings are decreased by a factor of two, i.e., $TF = 1/2$. This reduction in time and frequency spacings causes interference which is however purely imaginary due to the phase shift term $e^{j\frac{\pi}{2}(l+k)}$ [9]. The expression in (1) can be represented in matrix notation as follows [9]

$$\mathbf{s} = \mathbf{G}\mathbf{x}, \quad (3)$$

where the column vectors of \mathbf{G} are the sampled pulses $g_{l,k}(t)$ and \mathbf{x} is the transmitted symbol vector which is represented as

$$\mathbf{x} = [x_{1,1} \ x_{2,1} \ \cdots \ x_{L,1} \ x_{1,2} \ \cdots \ x_{L,K}]^T. \quad (4)$$

The expression in (3) is computed from Fast Fourier Transform (FFT) together with a polyphase network [9]. However, to simplify analytical investigations, the system is expressed as a

TABLE I
SIMULATION PARAMETERS

Parameters	ROV 1	ROV 2	ROV 3	ROV 4
Bandwidth	25 kHz			
Carrier frequency	32.5 kHz			
Water depth	1000 m			
TX height from sea-floor	4 m	4 m	5 m	7 m
RX height from sea-floor	998 m			
Number of TX, N_t	4			
Number of RX, N_r	100			
Subcarriers	256			
Delay spread	5.3 ms	5.3 ms	6.6 ms	9.2 ms
Modulation	64-QAM			
Turbo code rate	1/2			
Relative velocity	≈ 1.5 m/s			
Doppler frequency	≈ 32.5 Hz			
FBMC filter	Hermite prototype filter			
Filter overlapping factor	4			
FBMC spreading factor	16			

matrix multiplication. The received signal is expressed as

$$\mathbf{y} = \mathbf{D}\mathbf{x} + \mathbf{n} \quad (5)$$

$$= [y_{1,1} \ y_{2,1} \ \cdots \ y_{L,1} \ y_{1,2} \ \cdots \ y_{L,K}]^T,$$

where \mathbf{n} is the noise vector and \mathbf{D} is the transmission matrix which is defined as [9]

$$\mathbf{D} = \mathbf{G}^H \mathbf{G}. \quad (6)$$

For FBMC/OQAM, \mathbf{D} is affected by imaginary interference at the off-diagonal elements and hence is not an identity matrix in contrast to OFDM [9]. To obtain an identity matrix, only the real part of \mathbf{D} should be considered, i.e., $\Re\{\mathbf{D}\} = \mathbf{I}_{LK}$. For $L, K \rightarrow \infty$, the transmission matrix \mathbf{D} contains exactly $\frac{LK}{2}$ non-zero eigenvalues, each having a value of 2 [9]. This means that only $\frac{LK}{2}$ complex symbols can be transmitted. The spreading process consists of precoding the uncorrelated data symbols $\tilde{\mathbf{x}}$ using a unitary coding matrix \mathbf{C} to obtain the transmitted symbols as follows [9]

$$\mathbf{x} = \mathbf{C}\tilde{\mathbf{x}}. \quad (7)$$

The coding matrix \mathbf{C} is obtained by taking $\frac{K}{2}$ appropriate column vectors from a $K \times K$ Hadamard matrix and then spread with the symbols in the time domain [9]. This process is performed for all subcarriers to obtain the coding matrix, $\mathbf{C} \in \mathbb{R}^{LK \times \frac{LK}{2}}$. The imaginary interference is eliminated by choosing \mathbf{C} to satisfy the following condition [9]

$$\mathbf{C}^H \mathbf{D} \mathbf{C} = \mathbf{I}. \quad (8)$$

Finally, at the receiver end decoding is performed on the received symbols as follows

$$\tilde{\mathbf{y}} = \mathbf{C}^H \mathbf{y}. \quad (9)$$

V. MASSIVE MIMO

In massive MIMO the users communicate with the BS simultaneously over the same time and frequency resource and this results in significant improvement in spectrum efficiency [5]. In this work we focus on the uplink where data is transmitted from the users to the BS. In the uplink, the BS

requires channel state information (CSI) in order to decode the data received from multiple users. Hence the users transmit orthogonal pilots to the BS which in turn performs channel estimation based on the received pilot signals together with linear decoding techniques. Consider an uplink MU-massive MIMO system with a BS having N_r antennas and serving M users. For simplicity, we assume single-antenna users in the following formulations although these can be easily extended to multiple-antenna users. The baseband received signal vector at the BS can be expressed as follows [12]

$$\mathbf{y} = \mathbf{H}\mathbf{x} + \mathbf{n} = \sum_{m=1}^M \mathbf{h}_m x_m + \mathbf{n}, \quad (10)$$

where $\mathbf{h}_m \in \mathbb{C}^{N_r \times 1}$ is the channel vector between the BS and the m th user, $\mathbf{H} \triangleq [\mathbf{h}_1, \mathbf{h}_2, \dots, \mathbf{h}_M] \in \mathbb{C}^{N_r \times M}$ is the overall channel matrix, $\mathbf{x} \in \mathbb{C}^{M \times 1}$ is the transmitted symbol vector for all the users, $\mathbf{n} \in \mathbb{C}^{N_r \times 1}$ is the noise vector and $\mathbf{y} \in \mathbb{C}^{N_r \times 1}$ is the received signal vector. When the size of matrix \mathbf{H} increases, the channel hardening phenomenon occurs whereby the off-diagonal terms of the $\mathbf{H}^T \mathbf{H}$ matrix become smaller compared to the diagonal terms [13]. In this case the channel distortions are averaged out over time and frequency. It has been shown in numerous literatures that simple linear processing techniques such as minimum mean square error (MMSE) or zero-forcing (ZF) provide near-optimal performance in massive MIMO systems [14]. At the receiver, a linear detector is applied to the received signal vector \mathbf{y} to find an estimate of the transmitted symbol vector as follows [12]

$$\hat{\mathbf{x}} = \mathbf{A}^H \mathbf{y} = \mathbf{A}^H (\mathbf{H}\mathbf{x} + \mathbf{n}), \quad (11)$$

where \mathbf{A} is the $N_r \times M$ detection matrix and $\hat{\mathbf{x}} = [\hat{x}_1, \hat{x}_2, \dots, \hat{x}_M]^T$ is the $M \times 1$ signal vector which consists of the estimated data symbols transmitted from the M users. The m th element of the signal vector $\hat{\mathbf{x}}$ is represented as [12]

$$\hat{x}_m = \underbrace{\mathbf{a}_m^H \mathbf{h}_m x_m}_{\text{desired signal}} + \underbrace{\sum_{i \neq m}^M \mathbf{a}_m^H \mathbf{h}_i x_i}_{\text{inter-user interference}} + \underbrace{\mathbf{a}_m^H \mathbf{n}}_{\text{noise}}. \quad (12)$$

Depending on the type of linear detector used, either ZF or MMSE, the detection matrix \mathbf{A} is defined as

$$\mathbf{A} = \begin{cases} \mathbf{H}(\mathbf{H}^H \mathbf{H})^{-1}, & \text{for ZF} \\ \mathbf{H}(\mathbf{H}^H \mathbf{H} + \frac{\sigma_n^2}{\sigma_x^2} \mathbf{I}_M)^{-1}, & \text{for MMSE} \end{cases} \quad (13)$$

where σ_x^2 and σ_n^2 are the transmitted signal and noise variances respectively. The ZF linear detector selects the matrix \mathbf{A} to eliminate the inter-user interference regardless of the noise enhancement. In fact, it chooses \mathbf{A} such that $\mathbf{A}\mathbf{H} = \mathbf{I}$ [15].

VI. SIMULATION RESULTS

The physical setup of our UWA communication scenario is depicted in Fig. 1 while the relevant simulation parameters are summarized in Table 1. A statistical time-varying UAC is adapted in the simulations [16]. It is assumed that with each channel tap delay, the Doppler spread increases linearly from

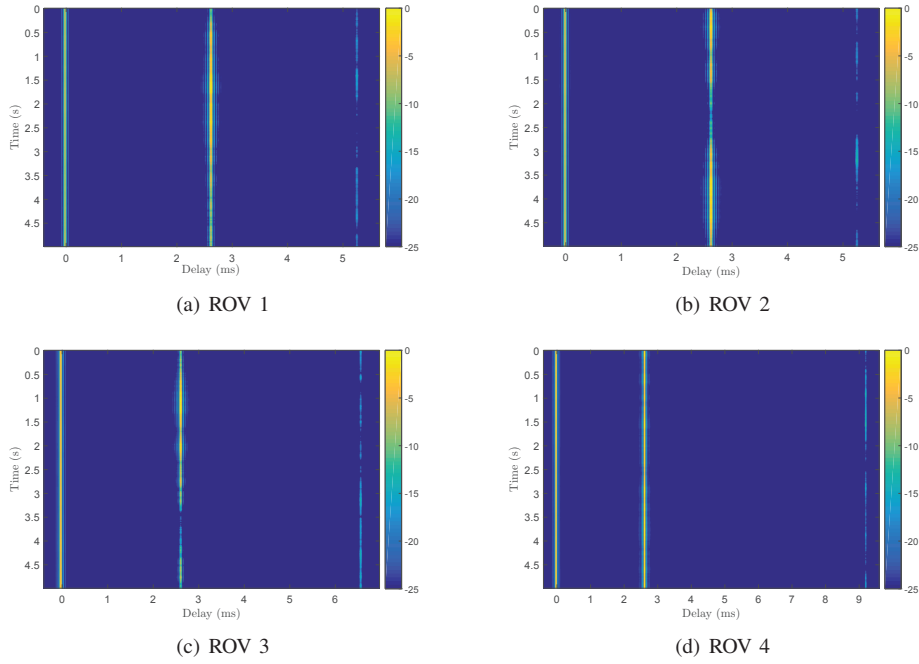


Fig. 2. Typical CIRs as observed between the BS and four ROVs

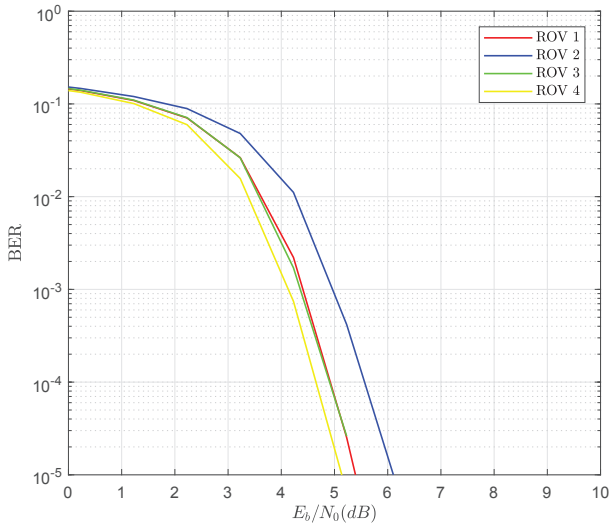


Fig. 3. BER performance of Turbo-coded massive MIMO-FBMC/OQAM systems in the UAC

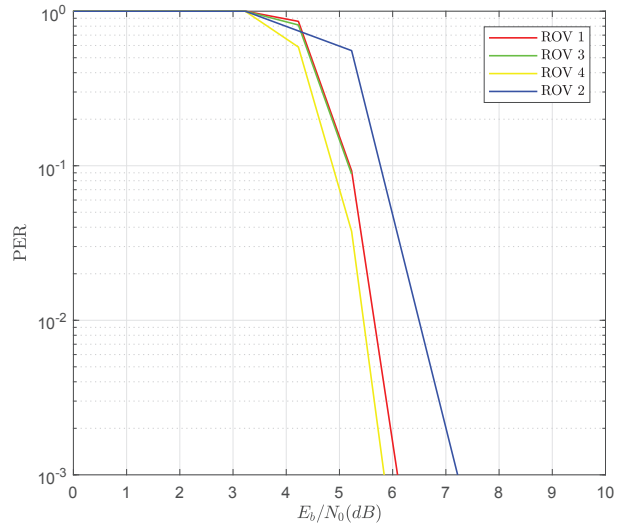


Fig. 4. PER performance of Turbo-coded massive MIMO-FBMC/OQAM systems in the UAC

0.5 Hz to 2 Hz. The typical channel impulse responses (CIRs) as observed by the four users (ROVs) are illustrated in Fig. 2.

To approximate a real-world UAC, colored noise is assumed in the simulations instead of additive white Gaussian noise (AWGN). The transmission of data is organized in packets for the FBMC/OQAM massive MIMO system. The time spreading performed in the FBMC/OQAM can result in interference between the packets and hence a zero guard interval is inserted between each of them. It is assumed that the four users send pilot signals and hence imperfect CSI is available for the BS to decode each user's data. For UWA communication,

the problem of pilot contamination is not as critical as in a terrestrial cellular communication system since the number of users is much less and there is only one BS which serves the users. Hence, orthogonal pilots can be easily assigned to each user. A ZF linear detector is used in the system to recover the transmitted symbols from each user at the BS.

Figures 3,4 and 5 show the performance of the four users in the UAC in terms of BER, PER and throughput respectively. The results show that the 4×100 FBMC/OQAM systems can achieve robust performance in the time-varying UAC due to the good time and frequency localization property of the FBMC's

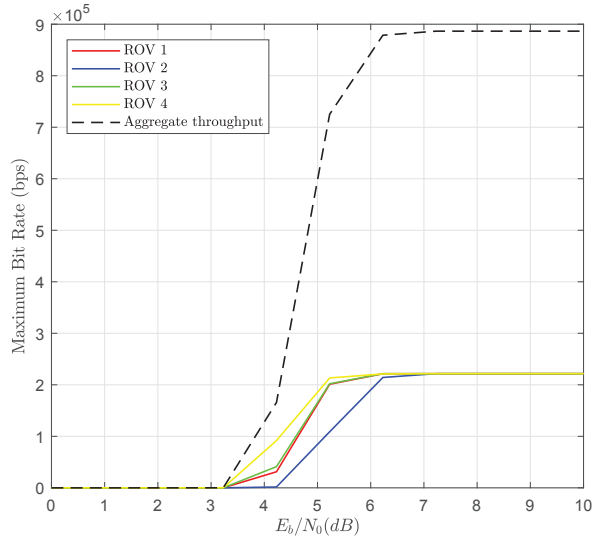


Fig. 5. Maximum achievable bit rates for the four ROVs in the UAC

prototype filter. The massive MIMO system allows all the ROVs (each equipped with four hydrophones) to transmit simultaneously over the same time and frequency resource and still achieve a very good error performance as can be observed in Fig. 3 and Fig. 4. In fact, in a massive MIMO FBMC system, the requirement of having approximately flat gain for the subcarriers can be relaxed [17]. This means that a smaller number of subcarriers can be used, hence reducing the latency or delay caused by the synthesis and analysis filter banks. A greater subcarrier spacing also implies that the system will be less susceptible to carrier frequency offsets. Furthermore, larger modulation orders can be used to further boost the bandwidth efficiency as linear combining of the signal components equalizes the channel gain across each subcarrier [17].

Fig. 5 shows the E_b/N_0 value that is required to achieve a given level of throughput for each user. It is to be noted that the guard intervals which are inserted in the FBMC/OQAM system cause a bandwidth efficiency loss of $\frac{1}{N+1}$ [9]. Therefore, the loss in bandwidth efficiency is 5.88% for a spreading length of 16. This loss is taken into account when computing the throughput in Fig. 5. We can infer that each ROV can reach their maximum throughput at a low E_b/N_0 value. Also, the fact that FBMC/OQAM is used instead of OFDM implies that each user achieves a higher bit rate since no bandwidth resources are wasted in the transmission of a CP. The overall aggregate throughput in this four-user massive MIMO system is approximately 886 kbps.

VII. CONCLUSION

Massive MIMO technology is expected to significantly improve the throughput and reliability not only in future terrestrial communication systems but also for UWA communication. The application of massive MIMO allows multiple ROVs

to be deployed simultaneously and the fact that they can all share the same time and frequency resources makes this technology very attractive for the UWA environment where the bandwidth is extremely limited, especially for long range links. We have seen in this work that all the users achieve very good error performance and high bit rates over a 1 km doubly-dispersive UAC using the FBMC/OQAM waveform shaping. Hence, FBMC/OQAM represents a better candidate than OFDM to be integrated in a massive MIMO system to satisfy the high data traffic and reliability demands of future underwater applications.

REFERENCES

- [1] M. Stojanovic and J. Preisig, "Underwater acoustic communication channels: Propagation models and statistical characterization," *IEEE Communications Magazine*, vol. 47, no. 1, pp. 84–89, Jan. 2009.
- [2] B. Li *et al.*, "MIMO-OFDM for high-rate underwater acoustic communications," *IEEE Journal of Oceanic Engineering*, vol. 34, no. 4, pp. 634–644, Oct. 2009.
- [3] M. Stojanovic, "MIMO OFDM over underwater acoustic channels," in *Proc. Systems and Computers 2009 Conf. Record of the Forty-Third Asilomar Conf. Signals*, Nov. 2009, pp. 605–609.
- [4] E. V. Zorita and M. Stojanovic, "Space-frequency block coding for underwater acoustic communications," *IEEE Journal of Oceanic Engineering*, vol. 40, no. 2, pp. 303–314, Apr. 2015.
- [5] A. Aminjavaheri and B. Farhang-Boroujeny, "UWA massive MIMO communications," in *OCEANS 2015 - MTS/IEEE Washington*, Oct 2015, pp. 1–6.
- [6] A. Aminjavaheri *et al.*, "Frequency spreading Doppler scaling compensation in underwater acoustic multicarrier communications," in *Communications (ICC), 2015 IEEE International Conference on*, Jun. 2015, pp. 2774–2779.
- [7] P. Amini *et al.*, "Filterbank multicarrier communications for underwater acoustic channels," *Oceanic Engineering, IEEE Journal of*, vol. 40, no. 1, pp. 115–130, 2015.
- [8] J. Gomes and M. Stojanovic, "Performance analysis of filtered multitone modulation systems for underwater communication," in *OCEANS 2009, MTS/IEEE Biloxi-Marine Technology for Our Future: Global and Local Challenges*. IEEE, 2009, pp. 1–9.
- [9] R. Nissel and M. Rupp, "Enabling low-complexity MIMO in FBMC-OQAM," in *2016 IEEE Globecom Workshops (GC Wkshps)*, Dec 2016, pp. 1–6.
- [10] R. Nissel, J. Blumenstein, and M. Rupp, "Block frequency spreading: A method for low-complexity MIMO in FBMC-OQAM," in *IEEE International Workshop on Signal Processing Advances in Wireless Communications (SPAWC), Sapporo, Japan*, 2017.
- [11] M. Stojanovic, "Underwater acoustic communications: Design considerations on the physical layer," in *Wireless on Demand Network Systems and Services, 2008. WONS 2008. Fifth Annual Conference on*. IEEE, 2008, pp. 1–10.
- [12] A. Azzadeh, R. Mohammadkhani, and S. V. A.-D. Makki, "BER performance of uplink massive MIMO with low-resolution ADCs," *arXiv preprint arXiv:1710.00335*, 2017.
- [13] T. L. Narasimhan and A. Chockalingam, "Channel hardening-exploiting message passing (CHEMP) receiver in large-scale MIMO systems," *IEEE Journal of Selected Topics in Signal Processing*, vol. 8, no. 5, pp. 847–860, Oct. 2014.
- [14] X. Li, E. Björnson, S. Zhou, and J. Wang, "Massive MIMO with multi-antenna users: When are additional user antennas beneficial?" in *2016 23rd International Conference on Telecommunications (ICT)*, May 2016, pp. 1–6.
- [15] F. A. de Figueiredo, J. P. Miranda, F. L. Figueiredo, and F. A. Cardoso, "Uplink performance evaluation of massive MU-MIMO systems," *arXiv preprint arXiv:1503.02192*, 2015.
- [16] F. X. Socheleau *et al.*, "A maximum entropy framework for statistical modeling of underwater acoustic communication channels," in *Proc. OCEANS 2010 IEEE - Sydney*, May 2010, pp. 1–7.
- [17] A. Farhang, N. Marchetti, L. E. Doyle, and B. Farhang-Boroujeny, "Filter bank multicarrier for massive MIMO," in *Vehicular Technology Conference (VTC Fall), 2014 IEEE 80th*. IEEE, 2014, pp. 1–7.